As a bonus, Mr. Fujii included a sketch of the encounter, confirming our claims that the published photograph had been reversed and that the tree in the foreground is a coconut palm.

IV. CONCLUSIONS

Using an eclipse map and some careful thought, we have deduced the conditions under which a widely circulated photograph was made. More important, what began as a simple and entertaining exercise in elementary analysis has become an even better lesson in caution and persistence.

[1]Timothy Ferris, *Spaceshots* (Pantheon, New York, 1984), photograph No. 45 and p. 131. Photograph used with permission of Akira Fujii.

[2]Eclipse map reproduced from U. S. Naval Observatory Circular No. 158, "Total solar eclipse of 16 February 1980." An excellent article concerning the eclipse is "Next February's total solar eclipse," Sky Telescope **58**, 4–5 [1979].

[3]See, for example, the Gallery Section of Sky Telescope **76**, 103–105 (1988).

[4]*Observer's Handbook*, edited by Roy L. Bishop (Royal Astronomical Society of Canada, Toronto, 1988), p. 61.

A square-well potential model to describe lambda-hypernuclei

P. B. Siegel and Mark Farrow-Reid[a)]

Physics Department, California State Polytechnic University, Pomona, Pomona, California 91768

(Received 7 April 1989; accepted for publication 10 July 1989)

In introductory quantum mechanics courses, square-well and step-function potentials are used in the Schrödinger equation to investigate properties of quantum mechanical systems, since they are simple enough for analytic solutions. Physical systems for which these closed-form solutions are applicable are excellent classroom examples. In this note, we present such a system: a Lambda particle bound inside a nucleus (Lambda-hypernuclei).

The available data on Lambda-hypernuclei come from strangeness-changing scattering experiments in which a neutron or proton in the nucleus is converted to a lambda particle. In practice, these reactions are observed when an incoming pion (or kaon) strikes the nucleus and a kaon (or pion) emerges as the outgoing scattered particle. By examining the kinematics of these reactions, the binding energy of the lambda particle in the nucleus can be measured, and from the angular distribution of the scattered kaon (or pion), the orbital angular momentum of the lambda with respect to the nuclear core can be determined as well. A summary of the most recent data and experimental techniques are given in Ref. 1. These include lambda particle binding energies for nuclei ranging from ^{12}C to ^{89}Y, and for lambda-(nuclear core) orbital angular momentum $l = 0$, $l = 1$, and $l = 2$ (see Fig. 1).

A standard approach to calculate the binding energies is to assume that the lambda moves in a mean-field potential due to the remaining neutrons and protons in the nucleus (i.e., the core).[2–4] This mean-field potential is inserted in the Schrödinger equation, and the resulting energy eigenvalues are compared with the experimental lambda binding energies. A commonly used ansatz for the nuclear mean-field is a Woods–Saxon potential:

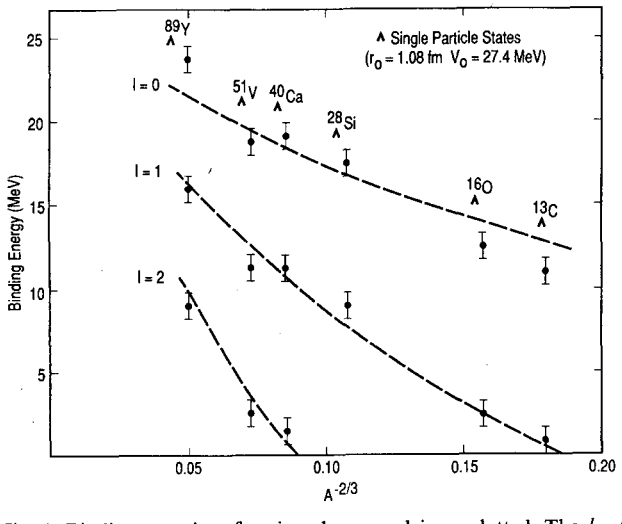

Fig. 1. Binding energies of various hypernuclei are plotted. The $l = 0$, $l = 1$, and $l = 2$ values signify the lambda-(core nucleus) orbital angular momentum. The dotted lines are the results of using a square-well potential with a depth of $V_0 = 27.4$ MeV, and a radius of $c = r_0 A^{1/3}$, where $r_0 = 1.08$ fm.

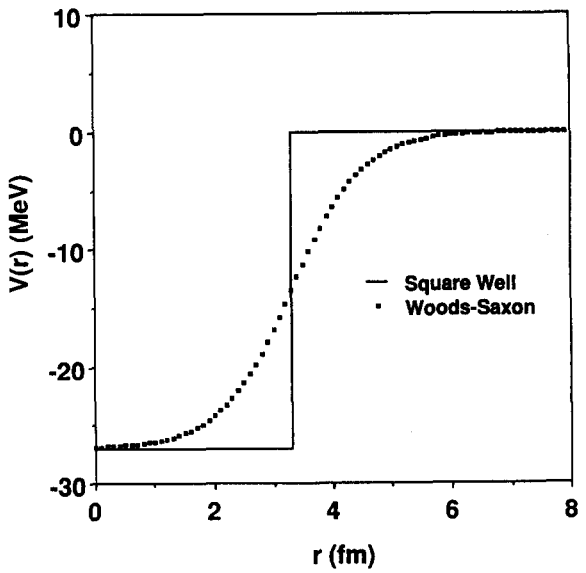

Fig. 2. A Woods–Saxon and a square-well potential are compared. Both potentials have the same strength, 27 MeV, and the same "radius parameter" c, 3.3 fm, which are appropriate values for ^{28}Si. The Woods–Saxon potential has a diffusivity parameter a of 0.6 fm.

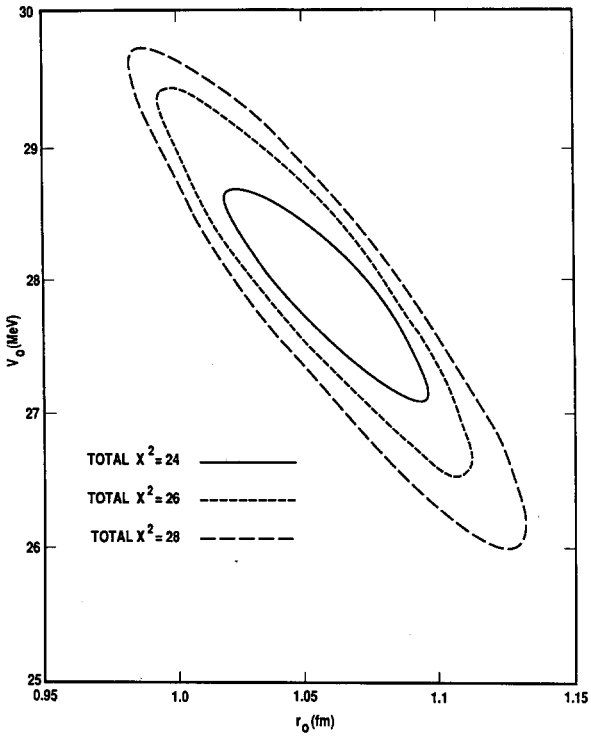

Fig. 3. Constant total chi-square ovals are plotted in the plane of the parameters r_0 and V_0. The total chi-square is defined as the sum over the 15 data points of

$$\chi^2 = \sum \left(\frac{(\text{Binding energy})_{\text{theory}} - (\text{Binding energy})_{\text{exp}}}{\text{Experimental uncertainty}} \right)^2.$$

$$V(r) = -V_0/\{1 + \exp[(r-c)/a]\}.$$

An excellent match to the data is obtained using $V_0 = 26$ MeV, $c = 1.1\,A^{1/3}$ fm, and $a = 0.6$ fm. Good fits to older data have also been obtained (see Ref. 4) using a three-dimensional square well. As we show below, the square-well potential fits the newer data as well. This is not surprising, since the shape of the Woods–Saxon potential is very similar to the three-dimensional square well. In fact, the Woods–Saxon potential approaches a square-well potential of radius c as the diffusivity parameter a approaches zero (see Fig. 2). Although not able to reproduce the binding energies to a high precision, the square well is easily solvable and thus has excellent application for the classroom. Its success is due to the properties of the lambda particle: It is chargeless, the nuclear spin–orbit interaction for the lambda is very small, and since there is only one lambda formed in the nucleus the Pauli exclusion principle does not apply.

The square-well potential is solved as an example in many undergraduate texts.[5] The $l = 0$, $l = 1$, and $l = 2$ energy levels, for example, are found to be solutions of the equations:

$$\epsilon \cot \epsilon = -\eta, \quad \text{for } l = 0,$$

$$\frac{\cot \epsilon}{\epsilon} - \frac{1}{\epsilon^2} = \frac{1}{\eta} + \frac{1}{\eta^2}, \quad \text{for } l = 1,$$

and

$$\frac{\tan \epsilon}{\epsilon}\left[3\left(\frac{1}{\eta}+1\right)\left(\frac{1}{\eta^2}+\frac{1}{\epsilon^2}\right) - \frac{1}{\epsilon}\right] = 3\left(\frac{1}{\eta}+1\right)\left(\frac{1}{\eta^2}+\frac{1}{\epsilon^2}\right) + \frac{1}{\eta}, \quad \text{for } l = 2.$$

The parameters ϵ and η are defined to be

$$\epsilon = \sqrt{2m_\Lambda (V_0 - |E|)/\hbar^2}\, c \quad \text{and} \quad \eta = \sqrt{2m_\Lambda |E|/\hbar^2}\, c$$

where $-V_0$ is the potential strength and c is the radius of the square well.

Choosing $c = r_0 A^{1/3}$, there are two parameters in the model, r_0 and V_0. For simplicity, we take the mass of the lambda m_Λ to be its rest mass, 1115.6 MeV. An excellent fit to the data is found when $V_0 = 27.4$ MeV and $r_0 = 1.08$ fm. These results are plotted along with the data in Fig. 1. Here, the binding energies are graphed as a function of $A^{-2/3}$, for comparison with Ref. 2. As can be seen, this simple model fits the data reasonably well. We also display the sensitivity to V_0 and r_0 in Fig. 3, where we have drawn constant chi-square ovals in the r_0–V_0 plane.

In conclusion, we point out that the three-dimensional square-well potential is a satisfactory model for describing the available lambda-hypernuclear data. This system is an excellent classroom example, since its solution can be treated at the undergraduate level. In addition to familiarizing the student with nuclear-size units, the success of the model demonstrates that

(a) The relation $c \propto A^{1/3}$ is verified, as well as setting the length scale of the nucleus;

(b) The lambda-nucleon force is short range;

(c) The lambda-nucleus mean-field potential is smaller than the nucleon–nucleus mean-field potential;

(d) The lambda-nuclear spin-orbit force is small.

We now have a physical system rich in pedagogical application, for which a simple square-well potential can be applied.

[a] This work was done to satisfy the requirement for the completion of the Bachelor of Science Degree.

[1] R. Chrien, "Studies of hypernuclei by associated production," Nucl. Phys. A **478**, 705–712 (1988).

[2] See D. J. Millener, C. B. Dover, and A. Gal, "Λ-nucleus single-particle potentials," Phys. Rev. C **38**, 2700–2708 (1988) and references therein for a recent discussion of the theoretical work on this subject.

[3] A. Gal, "Recent developments in hypernuclear spectroscopy," Nucl. Phys. A **479**, 97–113 (1988).

[4] L. E. Porter, "Light Λ^0-hypernuclei and the Lambda-nucleon potential," Am. J. Phys. **39**, 97–102 (1971).

[5] L. I. Schiff, *Quantum Mechanics* (McGraw-Hill, New York, 1968), pp. 83–88.